SMAR 2019 – Fifth Conference on Smart Monitoring,
Assessment and Rehabilitation of Civil Structures

SMAR 2019

A Proposed Approach for Processing and Analyzing Strain Data Collected In Full-Scale Accelerated Pavement Testing

Andrae FRANCOIS, Ayman ALI, Yusuf MEHTA [1]

[1] CREATEs at Rowan University, Glassboro, NJ, USA

Contact e-mail: mehta@rowan.edu

ABSTRACT: This study presents a general methodology to analyze strain data collected during accelerated pavement testing. Three instrumented, full-scale test sections were evaluated in this study. The sections had similar supporting layers however, different asphalt overlays were utilized on each test section. Section 1 contained a stone matrix asphalt overlay, section 2 contained a New Jersey high performance thin overlay, and section 3 contained a 9.5 ME Superpave mix placed on top of a binder rich intermediate course. The sections were loaded using a 60 kN, heavy vehicle simulator wheel load. Loading was applied uni-directionally at 8 km/h for 200,000 loading passes. The stiffness index and damage index parameters were computed using recorded strain measurements from all three sections, and their ability to distinguish the fatigue resistance of the asphalt overlays was evaluated. The APT strain data analysis procedure was successfully used to distinguish the fatigue resistance of asphalt overlays.

1 INTRODUCTION

Accelerated pavement testing (APT) has traditionally been used as means of understanding pavement response to loading under specific field conditions. It typically involves the application of a controlled wheel load to pavement structures in order to simulate long term in-service loading conditions in a condensed period of time Steyn (2009). The role of APT in pavement engineering has become more prominent over recent years due to the development of portable and non-portable accelerated pavement testing equipment that facilitate rapid field evaluation and performance comparison of pavements Ali and Mehta (2016). APT is generally centered on two main objectives: performance comparison of treatment(s) with a control section, and collection of performance data under controlled environmental and loading conditions to calibrate models Harvey (2009). In order to achieve these objectives of APT, appropriate instrumentation and collection of reliable continuous data is necessary.

Embedded stain gauges are generally used during APT to measure the dynamic material response of asphalt layers to moving traffic loads Hammons et al. (2007). The strain at the bottom of an asphalt layer in full scale test sections is typically monitored to capture the cracking failure mechanism (mainly load-associated fatigue cracking) of such layers. This is because load-related, strain accumulation beyond the allowable strength of asphalt mixtures typically leads to cracking Rodrigues et al. (2018). Cracking is considered the least understood distress in flexible pavements and generally leads to a rapid decrease in pavement service life. As a result, the measurement of strain at the bottom of the asphalt layer, assists APT users in quantifying or comparing the fatigue cracking potential or fatigue life of HMA layers in full-scale pavement sections.

The most common type of strain sensors utilized in APT facilities in the United States (US) are H-gauges (Figure 1). H-gauges are capable of measuring both longitudinal and transverse strain

depending on how they are oriented during installation. They consist of an electrical resistance strain gauge encased in an epoxy reinforced, fiber-glass strip that is attached to two transverse stainless steel anchors at each end of the fiber glass strip. The assembly of the epoxy reinforced, fiber-glass strip and transverse, stainless steel anchor bars combine to form an H-shape. H-gauges are used in APT facilities because of their ability to withstand high placement temperatures and compaction loads associated with pavement construction Hammons et al. (2007). H-gauges are also commonly utilized in APT facilities because the fiber glass strip in H-gauges has a comparable relative stiffness to asphalt mixtures which, allows for realistic pavement strain responses to be measured. Additionally, strain responses from H-gauges have been found to be highly repeatable regardless of loading conditions, pavement temperature, and sensor orientation Gokhale et al. (2009).

Figure 1. Typical H-gauge used in APT test facilities in the United States.

The measurement of reliable and repeatable pavement strain responses during APT provides the foundation for understanding the overall fatigue performance of pavements. This is because measured strains are indicators and predictors, of pavement fatigue life Gokhale et al. (2009). Some studies by Garcia and Thompson (2008) and Owende et al. (2001) have focused on developing efficient methods of processing strain data obtained from APT; mainly due to the large amount of strain data typically collected during APT. However, few studies have been aimed at establishing a method to analyze strain data obtained from APT. A testament to this fact is the lack of a standardized analysis method for evaluating the fatigue performance of full-scale sections in APT. The establishment of a standardized procedure for analyzing strain data is crucial because it will facilitate efficient and effective characterization of pavement responses and performance (i.e., correlation of strain data to fatigue life). Such a procedure is especially important as it will form the basis for establishing performance parameters through which the fatigue life of various full-scale pavement sections can be predicted, compared, and contrasted.

2 GOALS AND SCOPE

The overall goal of this paper is to present a general methodology for processing and analyzing strain measurements obtained from H-gauges embedded in full-scale, pavement sections. This study also aims at demonstrating the developed methodology by contrasting the fatigue characteristics of three flexible pavement sections constructed at the Rowan University Full-Scale Accelerated Pavement Testing Facility (RUAPTF).

3 EXPERIMENTAL PROGRAM AND DATA COLLECTION

3.1 Pavement Structure and Instrumentation of Test Sections

Strain data from three full-scale, pavement sections constructed at RUAPTF was collected as part of this study. The pavement sections were 9.2 m long by 3.6 m wide. Figure 2 presents a representative pavement structure (i.e., layers) for all three test sections. All sections had the same supporting layers or substructure (i.e., a Portland cement concrete (PCC) base, a granular

aggregate subbase, and compacted natural soil as a subgrade). However, different hot mix asphalt (HMA) overlays were utilized on each test section. On Section 1, a 76.2 mm thick Stone Matrix Asphalt (SMA) overlay was used, on Section 2, a 50.8 mm thick New Jersey High Performance Thin Overlay (NJHPTO) was used, and on Section 3, the overlay consisted of a 50.8 mm thick Superpave mix placed on top of a 25.4 mm thick Binder Rich Intermediate Course (BRIC).

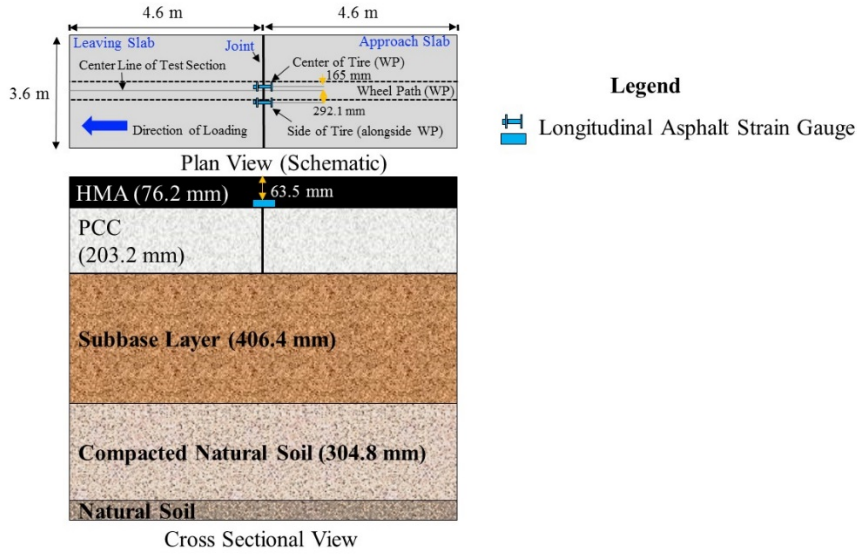

Figure 2. Pavement structure and instrumentation of test sections.

Each of the three test sections were instrumented with two H-type asphalt strain gauges that were placed 12.7 mm from the bottom of the asphalt overlay. The strain gauges were placed approximately 457 mm apart, at the joint, between the approach and leaving PCC slabs (Figure 2). One of the strain gauges was placed directly beneath the wheel path of one of the loading tires (dual-tire configuration) while the other was placed at the edge of the loading path. The length of each strain gauge was 100 mm and the gauges were capable of withstanding operational temperatures ranging between -20ºC to 180ºC.

3.2 Loading Program and Data Collection Frequency

A heavy vehicle simulator (HVS) was used to apply full-scale loading on all three pavement sections evaluated in this study. Each test section was subjected to a 60-kN load using a dual-tire, single-axle wheel configuration. The pressure in both tires was maintained at 758.4 kPa during loading. A total of 200,000 loading passes were applied on each test section at an 8 km/h, loading rate. Data from the embedded strain gauges was collected as HVS loading progressed on the test sections. A data acquisition system was used to collect strain measurements from the gauges during each load application. Strain data was collected at a frequency of 2,000 data points per second. The frequency at which strain measurements were recorded varied based on the stage of APT. For example, strain measurements were recorded at a high frequency (every 100 passes) during the application of the first 1,000 HVS passes, and the frequency reduced as loading progressed. Table 1 presents the loading passes at which strain measurements were recorded.

Table 1. HVS loading passes at which strain-time history pulses were recorded (sampling frequency)

Data Sampling Stage	Sampling Frequency
Below 1000 HVS Passes	Every 100th pass

1000 to 10,000 HVS Passes	Every 500th pass
10,000 to 20,000 HVS Passes	Every 1,000th pass
20,000 to 50,000 HVS Passes	Every 2,250th pass
50,000 to 100,000 HVS Passes	Every 10,000th pass
100,000 to 200,000 HVS Passes	Every 20,000th pass

4 ASPHALT STRAIN GAUGE ANALYSIS PROCEDURE

4.1 Step 1: Processing Strain Data

In the first step of the strain analysis procedure, strain measurements were obtained by converting the voltage signal recorded by the H-gauges embedded in a pavement section. Calibration factors, which were provided by the strain gauge manufacturers, were used to perform this task. The strain signal time history response was then filtered using a signal processing technique to remove any noise that was present in the data. It is suggested that a 25-data point moving average should be used to reduce the number of data points required to capture the strain response at a particular loading pass (when 10,000 data points are recorded). The process used to reduce the amount of data points per loading pass was found to accurately capture the trend of the full strain-time history response as shown in Figure 3a.

4.2 Step 2: Defining Phases of Strain-Time History Response

A representative strain-time history response for the test sections evaluated in this study is illustrated in Figure 3a. The strain-time history response obtained was similar to the strain response reported in previous studies by Qi et al. (2004) and Garg and Hayhoe (2001) for the longitudinal gauges subjected to dual wheel-single axle loads. That is, two consecutive cycles of compression (negative strain) and tension (positive strain); with little permanent deformation at the end of the strain response pulse. Based on the recorded strain responses, the second step of the asphalt strain data analysis procedure involved defining the various phases within the strain-time history response pulse for each recorded loading pass. To establish these phases, it was necessary to first identify critical points on the strain-time history response pulse (Figure 3b). The critical points were defined as local maximum or minimum points on the strain-time history pulse where the slope changed from positive to negative or vice versa. Using these turning points, four phases in the strain-time history pulse were defined (Figure 3b). Phase I represented the start of the strain time history pulse up until Turning Point 2 (TP2). This phase captured the initial compressive strain the overlay experienced at the joint when the load approached the joint from the approach slab. Phase II captured the tensile strain the overlay experienced when the load was directly on top of the joint (TP2 to TP3 in Figure 3). Phase III (Figure 3b) captured the compressive strain (TP3 to TP4) the overlay experiences as the load departed from the joint and Phase IV (TP4 to End Point (EP) in Figure 3b) captured the gradual increase in strain when the load no longer directly impacts joint (or slab) deflection. (i.e., as the load moved further away from the joint).

4.3 Step 3: Computing Maximum Tensile Strain and Strain Ratio Parameters

The phases defined in Step 2 of the procedure were utilized to determine two parameters which represented the strain response of the test sections during each recorded HVS pass. These parameters were the maximum tensile strain ($\varepsilon_{t\text{-}max}$) and the strain phase ratio (SP_R). The $\varepsilon_{t\text{-}max}$ was

computed as the absolute difference between the maximum tensile strain; TP3, and TP2 for each loading pass. The $\varepsilon_{t\text{-}max}$ represented the most critical tensile strain that the asphalt overlay experienced in a loading pass. Higher $\varepsilon_{t\text{-}max}$ values for a particular asphalt mixture, generally indicated that the HMA mixture was experiencing more damage. Thus, the $\varepsilon_{t\text{-}max}$ parameter was used to obtain insights related to the amount of damage being applied to an APT section during a particular loading pass. It is noted that other researchers Qi et al. (2004) and Huang et al. (2017) have successfully used $\varepsilon_{t\text{-}max}$ to compare the response of different asphalt overlays to various APT conditions such as: distance from the wheel path, load magnitudes, and loading rates.

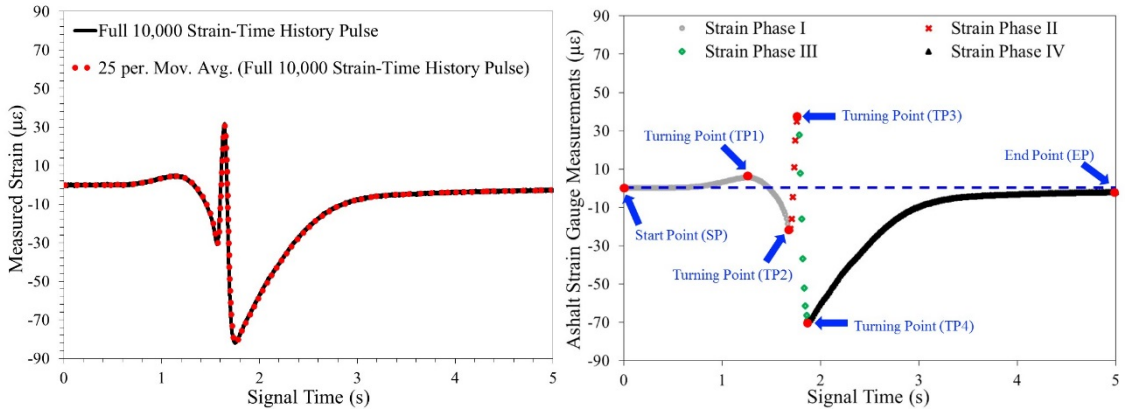

(a) (b)

Figure 3a. Example of measured and reduced strain-time history response obtained from a strain gauge embedded in one of the three test sections and Figure 3b. Critical points and critical strain phases.

The second parameter; the strain phase ratio, was computed as the ratio of compressive strain that represented the smaller of Phases I (i.e., |TP2 – TP1|, Figure 3b) and Phase III (i.e., |TP4 – TP3|) to the other compressive strain Phase (I or III) that represented the strain phase with the larger magnitude (Equation 1). This mathematical definition was employed to ensure that the SP_R values followed a logarithmic growth trend as the loading passes applied on the test sections increased; regardless of the strain response obtained from H-gauges. This was important because strain time history pulses in APT depend on the wheel loading configurations and asphalt mixtures types Qi et al. (2004) and Garg and Hayhoe (2001). Similar to $\varepsilon_{t\text{-}max}$, higher SP_R indicated that the asphalt layer was experiencing more damage at a particular loading pass. This is because the SP_R parameter captured the damage the asphalt overlays experienced during APT due to residual slab deflections at the joints (i.e., the compressive strain overlays experienced when the load approached and left joint).

$$SP_R = \begin{cases} \frac{Phase\ I}{Phase\ III} & if\ \ |SP2 - SP1| < |SP4 - SP3| \\ \frac{Phase\ III}{Phase\ I} & if\ \ |SP2 - SP1| \geq |SP4 - SP3| \end{cases} \quad (1)$$

4.4 Step 4: Determining Stiffness Index and Damage Index

After computing the maximum strain and strain phase ratio parameters from the measured strain data recorded during APT, two indices were determined. These indices were the stiffness index and the damage index. Equation 2 presents the mathematical representation of the stiffness index, which was computed for all recorded loading passes during APT. The stiffness index was conceptualized as parameter that would give some insights into the relative reduction in asphalt overlay stiffness directly over the joint, as loading progressed. This is because the stiffness index

incorporated the change in maximum strain the overlays experienced with time due to loading. Since in this study each test section consisted of a similar substructure and was subjected to similar loading conditions, the stiffness index was used as a comparative tool to draw conclusions about the relative fatigue resistance of the asphalt overlays.

$$Stiffness\ Index = \frac{1}{\varepsilon_{t-max}} \quad (2)$$

Prior to comuputing the damage index, the total damage (PD_i) applied to the overlays during APT due to loading and residual slab deflection was determined. The rate of change in the strain phase ratio was combined with the stiffness index to quantify the total damage (PD_i) applied to the overlays during each recorded wheel pass. The mathematical representation of the PD_i is shown in Equation 3. The Damage Index (DI) was then computed as the summation of damage applied for all loading passes as shown in Equation 4. The Damage Index can potentially be used as a comparative tool to assess the relative damage accumulation experienced in each asphalt overlay due to APT. This index is developed as a means to give an overall assessment of the relative fatigue resistance of the asphalt overlays.

$$PD_i = (Stiffness\ Index\ \times \Delta SP_R)_{pass\ i} \quad (3)$$

$$Damage\ Index\ (DI) = \sum PD_i \quad (4)$$

5 DEMONSTRAING THE PROPOSED STRAIN DATA ANALYSIS PROCEDURE

5.1 Maximum Tensile Strain and Strain Phase Ratio

The $\varepsilon_{t\text{-}max}$ and SP_R parameters were computed for all strain-time history pulses recorded during APT on all three pavement sections consisdered in this study. Figure 4a presents the computed $\varepsilon_{t\text{-}max}$ values obtained for all three sections and Figure 4b presents the SP_R values obtained for all sections. As evident from Figure 4a, the $\varepsilon_{t\text{-}max}$ computed for all three sections, followed a logarithmic growth trend, with the increase in number of loading passes applied. This trend was expected because an increase in applied loading passes typically amounts to an increase in permanent strain (or damage) within the asphalt layer of pavement sections. In addition, given the constant loading applied to all three pavement sections (i.e., 60 kN), it was deduced from Figure 4a that $\varepsilon_{t\text{-}max}$ parameter was able to differentiate between the asphalt overlays evaluated in this study. This is the case because $\varepsilon_{t\text{-}max}$ values for Section 1 (SMA) were higher than those for Section 2 (NJHPTO) which were also higher than $\varepsilon_{t\text{-}max}$ values for Section 3 (9.5ME & BRIC). Similar to the $\varepsilon_{t\text{-}max}$, the SP_R values illustrated in Figure 4b followed a logarithmic growth trend. That is, there was an increase in SP_R values when loading passes increased. As can be seen from Figure 4b, the SP_R parameter was also capable of differentiating between the three asphalt overlays.

5.2 Determining Stiffness Index and Damage Index

Figure 5a presents the stiffness index computed for all three pavement sections. The computed stiffness index values followed a logarithmic decay trend. This trend was expected because the stiffness index values were computed directly from the maximum tensile strain, which followed a logarithmic growth trend (i.e., $\varepsilon_{t\text{-}max}$ increased as loading passes increased). The trend observed is similar to what is typically observed during laboratory assessment of asphalt mixture fatigue properties. This is significant because existing literature attributes the reduction in moduli values for an asphalt mixture to damage accumulation as loading cycles are applied. For instance, Shen and Carpenter (2007) reported that modulus reduction is closely associated with the overall fatigue life of the asphalt layer. Therefore the observations from Figure 5, along with supporting

literature indicate that the use of stiffness index in comparing the relative fatigue resistance of full-scale instrumented asphalt pavement layer is practical (i.e., easy to compute) and may correlate to the fatigue performance of asphalt mixtures.

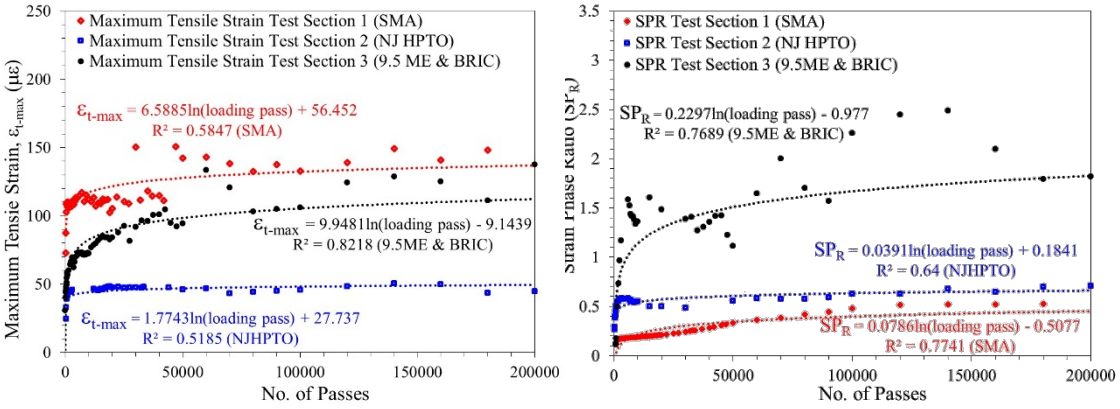

(a) (b)

Figure 4a. Maximum tensile strain (ε_t-max) and Figure 4b. Strain phase ratio (SP_R) versus number of applied HVS loading passes for all three sections.

Figure 5b presents the damage index (DI) computed using Equation 4 for each pass. The DI values shown in Figure 5b increased at different rates for the different asphalt overlays (or sections). Additionally, by comparing the accumulated damage after applying a certain number of loading passes (for example 160,000 loading passes), it can be observed that Section 3 (9.5ME & BRIC) had the highest accumulated damage, followed by Section 2 (NJHPTO) and Section 1 (SMA), respectively. These results indicated that Section 1 had the best fatigue cracking resistance followed by Section 2 and Section 3, respectively. This is the case because for Section 3 to reach the same level of damage seen for Section 3 after applying 160,000 passes, the application of more loading cycles is required on this section (Section 1). Based on these observation, it was deduced that the rate of increase in the damage index (DI) for all three sections was adequately able to differentiate the fatigue resistance of the asphalt overlays considered in this study.

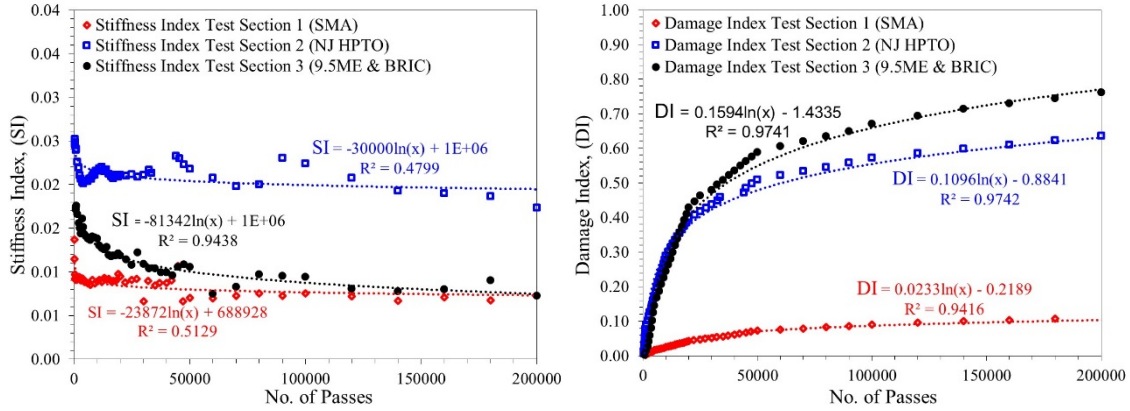

(a) (b)

Figure 5a. Computed stiffness index and Figure 5b. Damage index for all loading passes.

6 SUMMARY AND CONCLUSIONS

Based on the strain data collected and the subsequent analysis procedure using the collected data, the following conclusions were drawn:

- General APT strain data processing and analysis approach presented in study was successfully used to rank all three sections. This is the case because the computed analysis indices (stiffnes index and damage index) were able to distinguish between the sections.
- Results presented in this paper are only for the three full-scale pavement sections (i.e., three different overlays) evaluated in this study. Validation of the presented analysis approach and parameters is required using strain gauge data from APT on other sections.

7 REFERENCES

Ali, A. W., and Y. Mehta, 2016, Heavy vehicle simulator and accelerated pavement testing facility at Rowan University. *5th International Conference on Accelerated Pavement Testing Conference, Transportation Research Board*. Costa Rica.

Garcia, G. and M.R. Thompson, 2008, Strain and pulse duration considerations for extended life hot mix asphalt pavement design. *Transportation Research Record: Journal of the Transportation Research Board*, 2087: 3–11.

Garg, N. and G.F. Hayhoe, 2001, Asphalt concrete strain responses at high loads and low speeds at the national airport pavement test facility (NAPTF). *Airfield Pavement Specialty Conference, American Society of Civil Engineers*. Chicago, I.L.

Gokhale, S., T. Byron, S. Iyer, and B. Choubane, 2009, Evaluation of pavement strain gauge repeatability: results from accelerated pavement testing. *Transportation Research Record: Journal of the Transportation Research Board*, 2094: 30-40.

Hammons, M. I., D. Timm, and J. Greene, 2007, Instrumentation Data Interpretation. *Florida Department of Transportation State Materials Office*, Gainesville, F.L.

Harvey, J. T., 2009, Transportation research circular E-C139: Accelerated pavement testing experiment to assess the use of modified binders to limit reflective cracking in thin asphalt overlays. *Transportation Research Record: Journal of the Transportation Research Board*, 11-31.

Huang, Y., L. Wang, and H. Xiong, 2017, Evaluating pavement response and performance under different scales of APT facilities. *Innovations in Characterization and Modeling of Road Materials and Pavements*, 18: 159-169.

Owende, P. M. O., A. M. Hartman, S. M. Ward, M.D. Gilchrist, and M. J. O'Mahony, 2001, Minimizing distress on flexible pavements using variable tire pressure. *Transportation Research Record: Journal of the Transportation Research Board*, 127(3): 254-262.

Qi, X., T. Mitchell, K. Stuart, J. Youtcheff, K. Petros, T. Harman, and G. Al-Khateeb, 2004, Strain responses in ALF modified-binder pavement study. *2nd International Conference on Accelerated Pavement Testing, Transportation Research Board.* Minneapolis, M.N.

Rodrigues de Mello, L. G., M. Muniz de Farias, and K.E. Kaloush, 2018, Using damage theory to analyze fatigue of asphalt mixtures on flexural tests. *International Journal of Pavement Research and Technology*, 11(4).

Shen, S., and S. Carpenter, 2007, Dissipated energy concepts for HMA performance: fatigue and healing. *Federal Aviation Administration (FAA)*, Publication DOT 05-C-AT-UIUC-COE.

Steyn, W., 2009, Transportation research circular E-C139: Use and application of accelerated pavement testing in pavement preservation treatments. *Transportation Research Record: Journal of the Transportation Research Board*, 49-58.